Geomechanics and Engineering, *Vol. 40, No. 6 (2025) 411-421*
https://doi.org/10.12989/gae.2025.40.6.411

Analytical solution of one dimensional migration of suspended particles based on stochastic model

Peng Zhu, Yan Wang*, Chuancheng Xue and Ganbin Liu

School of Civil, Environmental Engineering and Geography Science, Ningbo University, Ningbo 315211, China

(*Received March 15, 2023, Revised February 10, 2025, Accepted March 6, 2025*)

Abstract. Based on the suspended particles (SPs) migration model considering the release effect, combined with the stochastic model, the analytical solution in the case of instantaneous injection was obtained. In the stochastic model, the probability density function (PDF) was characterized using the lognormal, bimodal lognormal and the joint lognormal distribution formulas. The single or double stochastic parameters were considered to study the migration characteristics of the SPs. When the single parameter deposition coefficient follows the lognormal distribution, the peak concentration of SPs increases with the standard deviation. As for the case of average pore velocity following the lognormal distribution, the peak concentration decreases and the corresponding time advances with the standard deviation increasing, and the breakthrough curves (BTCs) become more asymmetrical. When the deposition coefficient obeys the bimodal lognormal distribution, the peak concentration increases with increasing the proportion of low deposition coefficient. When the average pore water velocity follows the bimodal lognormal distribution, the peak concentration changes with the variation of the proportion of low pore water velocity, while the corresponding time is almost unchanged. When the double stochastic parameters follow the lognormal distribution, the peak concentration of SPs increases with the decrease of correlation coefficient and the BTCs become relatively symmetrical, with less trailing phenomenon. With the increase of migration distance, the peak concentration decreases and the time corresponding to the peak concentration of SPs increases.

Keywords: analytical solution; deposition; one dimensional migration; release; stochastic model; suspended particle

1. Introduction

The migration of suspended particles (SPs) occurs in many underground engineering fields (Babakhani *et al.* 2017, Zhu *et al.* 2021, Cui *et al.* 2022, Ding *et al.* 2022). For example, in the process of oil exploitation, improper control of SPS content in waste water reinjection can cause reservoir damage and reduce recovery efficiency (Cui *et al.* 2019). The heavy metal pollutants also can be adsorbed on particles and further diffuse along with surface runoff and groundwater (Bai *et al.* 2021, Qi *et al.* 2021), causing detriment to the ecological environment (Hossini *et al.* 2022). Due to the migration and deposition of suspended particles, the underground infiltration system can be blocked, making it difficult for rainwater to recharge the aquifer (Wang *et al.* 2012). The root cause of the above problems lies in the lack of understanding of the mechanism of migration and deposition of SPs in porous media. Therefore, studying the migration characteristics of SPS is vital important.

Many scholars have studied the migration and deposition of suspended particles (Sim and Chrysikopoulos 1998, Hosseini and Tosco 2013, Haque *et al.* 2017, Dong *et al.* 2018, Ma *et al.* 2018). The clean-bed filtration theory (CFT) is widely used to study the deposition behavior of SPs in porous media (Taghavy *et al.* 2018, Lin *et al.* 2022). This theory presents a first-order SPs deposition term, which makes an exponential distribution of the deposition of SPs in porous media with depth (Tufenkji and Elimelech 2005a, Bradford *et al.* 2013, Braga and Filion 2022). Over the past years, an increasing number of studies have indicated that the clean bed filtration theory often fails to accurately describe the deposition distribution of SPs under unfavorable deposition conditions, especially when repulsive electrostatic interactions exist between colloids and particle surfaces (Tufenkji and Elimelech 2005a). In this case, the retained SPs often exhibit a hyper-exponential distribution (Bradford and Leij 2018, Zou *et al.* 2019a). Katzourakis and Crysikopoulos (2019) considered the deposit with two-site kinetics and effectively described the transport of two clays in a horizontal column. Johnson *et al.* (2018) studied the transport of carboxylate-modified polystyrene latex microspheres (CML) in glass beads and found that CML in the column exhibited a hyper-exponential distribution under condition of colloid-collector repulsion. Stochastic models were established to describe the phenomenon of hyper-exponential distribution (Tufenkji and Elimelech 2004, 2005b). In the stochastic model, various probability density functions can be used to characterize deposition coefficient (Tufenkji *et al.* 2003).

In addition, some scholars also found that the migration of SPs could be affected by various physical and chemical factors in porous media (Bai *et al*. 2016). Abdel-Salam and Chrysikopoulos (1994) studied the effect of fracture aperture and deposition coefficient on SPs transport in

*Corresponding author, Professor
E-mail: wanyang@nbu.edu.cn

ISSN: 2005-307X (Print), 2092-6219 (Online)

saturated fractures, and the results indicated that SPs concentrations decreased with increasing deposition coefficient and decreasing fracture aperture. Also, the aquifer boundary conditions significantly influenced the migration of SPs (Sim and Chrysikopoulos 1999, James and Chrysikopoulos 2003). Furthermore, SPs deposited on the surface of solid matrix could be released (Bradford *et al*. 2013, Wang *et al.* 2022). Chen *et al*. (2017) studied the effect of flow velocity increment on particle release in porous media and the results indicated that release rates of particles increased with both flow velocity and velocity increment. Zou *et al*. (2019b) investigated the physical clogging of porous media by injecting particles and found that the continuous hydraulic gradient caused the fine SPs released, and the breakthrough curve also demonstrated this result. Bai *et al*. (2017) considered the deposition and release effect of SPs in the deposition kinetic equation, and analyzed the effect of temperature on the deposition coefficient and release coefficient by experiments. In order to better describe the migration properties of SPs in saturated porous media, the release effect of SPs should be considered in classic convection-dispersion equation.

The purpose of the current study is to present analytical solutions to SPs migration models that account for the release effect, instantaneous sources, and stochasticity of parameters. Lognormal distribution probability density functions, bimodal lognormal distribution probability density functions, and the joint probability density function were introduced to characterize stochastic variables including deposition coefficient and pore water velocity, while also considering their coupled effects on SPs migration. Thus, not only the re-release effect of the SPs was considered, but also the stochasticity of the deposition coefficient and pore water velocity were considered to study the behavior of the migration of SPs, providing further understanding of the stochasticity inherent in field conditions.

2. Governing equation

The classic models of suspended particle migration include: suspended particle mass balance equation and suspended particle deposition kinetic equation, which have been widely used in the field of groundwater environmental protection and other fields. In the classical model, it is assumed that the SPs are irreversibly deposited on the matrix. However, previous studies have shown that the deposition and release of SPs occur at the same time, leading to a nonnegligible discrepancy between theoretical results and experimental results (Tufenkji *et al*. 2003, Shapiro and Bedrikovetsky 2010), indicating that the classical model has certain limitations and it is necessary to modify the classical model. Considering the deposition and re-release process of SPs in the kinetic equation of SPs can better describe the migration process of SPs in porous media. The schematic diagram of migration of SPs in porous media is shown in Fig. 1.

The mass balance equation and the deposition kinetic equation of SPs in porous media considering the effect of

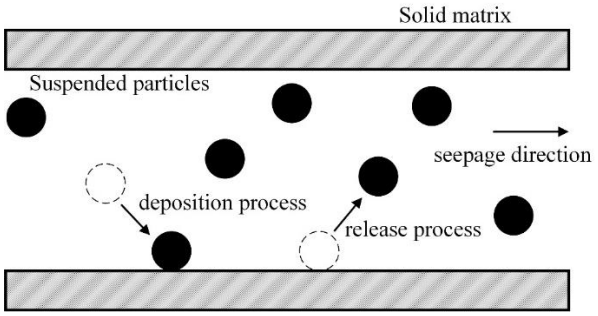

Fig. 1 Sketch of suspended particle migration process

deposition and re-release can be written as (Bradford and Toride 2007, Bai *et al.* 2017)

$$\frac{\partial C(x,t)}{\partial t} = D\frac{\partial^2 C(x,t)}{\partial x^2} - v\frac{\partial C(x,t)}{\partial x} - \frac{\rho_s}{\theta}\frac{\partial S(x,t)}{\partial t} \tag{1}$$

where v is the average pore water velocity [LT^{-1}], θ is the volumetric water content, ρ_s is the dry bulk density of the porous medium [ML^{-3}], t is the elapsed time [T], C is the concentration of SPs [ML^{-3}], S is the concentration of SPs deposited in the solid matrix [ML^{-3}], D is the dispersion coefficient [L^2T^{-1}], and x is the migration distance [L].

The corresponding SPs mass balance equation for the solid phase is given as

$$\frac{\rho_s}{\theta}\frac{\partial S(x,t)}{\partial t} = k_d C(x,t) - k_r\frac{\rho_s}{\theta}S(x,t) \tag{2}$$

where k_d and k_r is the deposition and release coefficients respectively [T^{-1}].

$$C(x,0) = 0, 0 \le x \le \infty \tag{3}$$

$$C(0,t) = \frac{M}{Q}\delta(t) \tag{4}$$

$$\frac{\partial C(\infty,t)}{\partial x} = 0 \tag{5}$$

$$S(x,0) = 0 \tag{6}$$

where M is the injected particle mass [M], and Q is the flowrate [L^3T^{-1}].

3. Model solving

The Laplace transforms with respect to time t in *C(x,t)* and *S(x,t)* are defined as

$$C(x,t) = \frac{1}{2\pi i}\int_\Gamma e^{pt}\overline{C}(x,p)dp \tag{7}$$

$$S(x,t) = \frac{1}{2\pi i}\int_\Gamma e^{pt}\overline{S}(x,p)dp \tag{8}$$

where p is the Laplace transform variable.

Combining the Laplace transforms with respect to time t in Eqs. (1) and (2) and Eqs. (3) and (6) yields

$$p\overline{C} = D\frac{\partial^2 \overline{C}}{\partial x^2} - v\frac{\partial \overline{C}}{\partial x} - k_d \overline{C} + k_r \frac{\rho_s}{\theta}\overline{S} \tag{9}$$

$$\frac{\rho_s}{\theta} p \cdot \overline{S} = k_d \overline{C} - k_r \frac{\rho_s}{\theta}\overline{S} \tag{10}$$

Simplifying Eqs. (9) and (10) yields

$$D\frac{\partial^2 \overline{C}}{\partial x^2} - v\frac{\partial \overline{C}}{\partial x} - p(1+\frac{k_d}{p+k_r})\overline{C} = 0 \tag{11}$$

Performing Laplace transform to the Eq. (4) yields

$$\overline{C}(0, p) = \frac{M}{Q} \tag{12}$$

Combining Eqs. (11) and (12) yields

$$\overline{C} = \frac{M}{Q}\exp\left\{\frac{x}{2D}\left[v - \sqrt{v^2 + 4Dp\left(1+\frac{k_d}{p+k_r}\right)}\right]\right\} \tag{13}$$

Applying the inverse Laplace transform definition and property

$$C(x,t) = \frac{1}{2\pi i}\int_\Gamma e^{pt}\overline{C}(x, p)dp \tag{14}$$

$$\frac{2}{\sqrt{\pi}}\int_0^\infty e^{-\xi^2-\mu^2/\xi^2} d\xi = e^{-2\mu} \tag{15}$$

where Γ is the given path in the specified complex s plane.

Based on Eqs. (13) and (15) can be expressed as

$$\overline{C} = \frac{2}{\sqrt{\pi}}\cdot\frac{M}{Q}e^a \cdot \int_0^\infty \exp\left\{-\xi^2 - a^2\left[1+b^2 p(1+\frac{k_d}{p+k_r})\right]/4\xi^2\right\} d\xi \tag{16}$$

where $a = \dfrac{vx}{2D}, b^2 = \dfrac{4D}{v^2}$

Substituting Eq. (16) into Eq. (14) yields

$$\frac{Q}{M}\overline{C} = \frac{2e^a}{\sqrt{\pi}}\cdot\int_0^\infty \exp(-\xi^2 - \frac{a^2}{4\xi^2})\cdot F \tag{17}$$

$$F = \exp\left[-k_r t - \frac{a^2 b^2}{4\xi^2}(k_d - k_r)\right]\cdot R \tag{18}$$

$$R = \frac{1}{2\pi i}\int_\Gamma \exp(-\frac{\beta^2}{\xi^2}\varphi)\exp\left[\varphi t + \frac{\alpha^2}{\varphi}\right] d\varphi \tag{19}$$

where $\alpha^2 = \dfrac{a^2 b^2 k_d k_r}{4\xi^2}, \beta^2 = \dfrac{a^2 b^2}{4}, \varphi = p + k_r$, ξ and φ are dummy variables.

$$\frac{Q}{M}\overline{C} = \frac{2e^a}{\sqrt{\pi}}\cdot\int_0^\infty \exp(-\xi^2 - \frac{a^2}{4\xi^2})\cdot F \tag{20}$$

$$f(t) = L^{-1}\exp(\frac{\alpha^2}{\varphi}) \tag{21}$$

According to the time-shift theorem

$$f(t-b)u(t-b) = L^{-1}e^{-bp}F(p), (b>0) \tag{22}$$

$$R = f(t-\frac{\beta^2}{\xi^2})u(t-\frac{\beta^2}{\xi^2}) \tag{23}$$

where $u(t-\dfrac{\beta^2}{\xi^2})$ is the unit step function, therefore

$$R = \begin{cases} 0 & , \ t < \dfrac{\beta^2}{\xi^2} \\ f(t-\dfrac{\beta^2}{\xi^2}) & , \ t > \dfrac{\beta^2}{\xi^2} \end{cases} \tag{24}$$

Only if $t > \dfrac{\beta^2}{\xi^2}$, and $\xi > x/2\sqrt{Dt}$, R can have actual meaning.

According to the derivative property of Laplace transform

$$R = f(t-\frac{\beta^2}{\xi^2})u(t-\frac{\beta^2}{\xi^2}) \tag{25}$$

where $G(\varphi) = \dfrac{1}{\varphi}\exp(\dfrac{\alpha^2}{\varphi})$, $g(t) = I_0(2\sqrt{\alpha^2 t})$ and $g(0) = 1$, therefore

$$f(t) = L^{-1}\varphi[\frac{1}{\varphi}\exp(\frac{\alpha^2}{\varphi})] = \sqrt{\frac{\alpha^2}{t}}\cdot I_1(2\alpha\sqrt{t}) + \delta(t) \tag{26}$$

where I_0 and I_1 are modified Bessel functions.

Substituting Eq. (26) into Eq. (24) results in

$$R = f(\lambda) = \sqrt{\frac{\alpha^2}{\lambda}}\cdot I_1(2\alpha\sqrt{\lambda}) + \delta(\lambda) \tag{27}$$

where $\lambda = t - \dfrac{\beta^2}{\xi^2}$.

Combining Eqs. (17) and (27) generates the concentration of SPs in porous media under the condition of instantaneous injection

$$C = \frac{2Me^a}{Q\sqrt{\pi}}\int_{x/2\sqrt{Dt}}^\infty \exp(-\xi^2 - \frac{a^2}{4\xi^2})\cdot\exp[-k_r t - \frac{a^2 b^2}{4\xi^2}(k_d - k_r)]\cdot R d\xi \tag{28}$$

4. Stochastic model

The deposition coefficient is assumed to be constant in the Eqs. (1) and (2), but in practice, the deposition coefficient is a hyper-exponential distribution (Yuan and Sin 2011, Bradford and Leij 2018, Johnson *et al*. 2020). In the stochastic model, the probability density function is

used to represent the deposition coefficient. If the deposition coefficient is defined as stochastic, we assumed a lognormal distribution probability density function as (Tufenkji *et al.* 2003, Bradford and Toride 2007)

$$F(k_d)=\frac{1}{k_d\sigma_d\sqrt{2\pi}}\exp[-\frac{Y_d^2}{2}] \quad (29)$$

$$Y_d=\frac{\ln(k_d)-\mu_d}{\sigma_d} \quad (30)$$

where μ_d and σ_d are the mean value and standard deviation of the lognormal distribution probability density function, respectively, and $\mu_d=\ln(\bar{k}_d)-0.5\sigma_d^2$, $\bar{k}_d$ is the ensemble average of k_d.

The bimodal lognormal distribution developed from Eq. (29) can describe more complex particle migration problems

$$F(k_d)=\frac{f_{low}}{k_d\sigma_{low}\sqrt{2\pi}}\exp[-\frac{Y_{d,low}^2}{2}]+\frac{f_{high}}{k_d\sigma_{high}\sqrt{2\pi}}\exp[-\frac{Y_{d,high}^2}{2}] \quad (31)$$

where f_{low} and f_{high} are the proportions of the two deposition coefficients respectively, and $f_{low}=1-f_{high}$. When σ_{low} and σ_{high} approach zero, Eq. (31) can be written as

$$F(k_d)=f_{low}\delta(k_d-k_{low})+f_{high}\delta(k_d-k_{high}) \quad (32)$$

where k_{low} and k_{high} are the two deposition coefficients, σ_{low} and σ_{high} are the corresponding standard deviations respectively.

From the probability density function $F(k_d)$, the average suspended particle concentrations in aqueous and solid phases at given depth and time can be determined

$$C^*(x,t)=\int_0^\infty C(x,t,k_d)F(k_d)dk_d \quad (33)$$

$$S^*(x,t)=\int_0^\infty S(x,t,k_d)F(k_d)dk_d \quad (34)$$

where *S(x,t)* can be obtained according to Eq. (2)

$$S(x,t,k_d)=k_d\cdot\frac{\theta}{\rho_s}\cdot\int_0^t C(x,t)\exp[-k_r(t-\tau)]d\tau \quad (35)$$

If the release coefficient k_r or the average pore water velocity v is stochastic and other parameters are constant, k_r or v also can be described by a probability density function.

If both k_r and k_d are subjected to the lognormal distribution, then the joint probability density function is defined as

$$F(k_d,k_r)=\frac{1}{2\pi k_d k_r\sigma_d\sigma_r\sqrt{1-\rho_{dr}^2}}\exp[-\frac{Y_r^2-2\rho_{dr}Y_rY_d+Y_d^2}{2(1-\rho_{dr}^2)}] \quad (36)$$

where ρ_{dr} is the correlation coefficient between Y_d and Y_r, which is defined as

$$\rho_{dr}=\int_0^\infty\int_0^\infty Y_rY_dF(k_d,k_r)dk_ddk_r \quad (37)$$

when Y_d and Y_r are completely correlated, ρ_{dr}=1; when Y_d and Y_r are not correlated, ρ_{dr} =0; and when they are negatively correlated, ρ_{dr}=-1.

From the probability density function $F(k_d,k_r)$, the average suspended particle concentrations in aqueous and solid phases at given depth and time can be determined

$$C^*(x,t)=\int_0^\infty\int_0^\infty C(x,t;k_d,k_r)F(k_d,k_r)dk_ddk_r \quad (38)$$

$$S^*(x,t)=\int_0^\infty\int_0^\infty S(x,t;k_d,k_r)F(k_d,k_r)dk_ddk_r \quad (39)$$

Similarly, if both k_r and v are subjected to lognormally distribution, the joint probability density function can be utilized in the same way.

5. Model analysis

The model parameters are selected from the reference (Bradfrod and Toride 2007). To better observe the migration characteristics of SPs, the trend of the curves in Fig. 2 can be explained by the standard deviation in the probability density function Eq. (29). When the probability density function is used to represent the deposition coefficient, the parameters are shown in Table 1.

The average pore water velocity v and the release coefficient k_r are assumed to be constant, and the SPs migrate along the x-axis direction. At the position x = 10, 15 and 20 cm, the variation curves of the SPs concentration with elapsed time at different standard deviation σ_d are show in Fig. 2.

Fig. 2 shows that the BTCs of SPs when σ_d is 0, 0.5, and 1. When $\sigma_d=0$, the stochastic model can degenerate into a modified model Eqs. (1) and (2) in which the deposition coefficient is a constant. When σ_d increases, the lognormal distribution is more asymmetric and the distribution range of deposition coefficients increase. The frequency of low and high deposition coefficient became higher, and the mean value of the lognormal distribution and the average deposition coefficient decreased, that is, fewer SPs were deposited in porous media. For instance, as shown in Fig. 2(a), the peak concentration of SPs increased from 0.0358, 0.0393 to 0.0479 mg/ml with increasing σ_d from 0, 0.5 to 1 respectively at x=10 cm. The time to reach the concentration peak is delayed with increasing x, and the corresponding concentration peak decreases since more SPs are deposited in porous media.

As the time elapses, the SPs can migrate to farther location, and the peak concentration of SPs turns to decrease. With increasing σ_d, the average deposition coefficient decreases, and the peak concentration increases accordingly.

When applying the probability density function to represent the average pore water velocity, the related parameters are shown in Table 2. The deposition coefficient and the release coefficient are assumed constants, and the SPs migrate along the x-axis direction. At the location x=10, 15, and 20 cm, the variation curves of the suspended

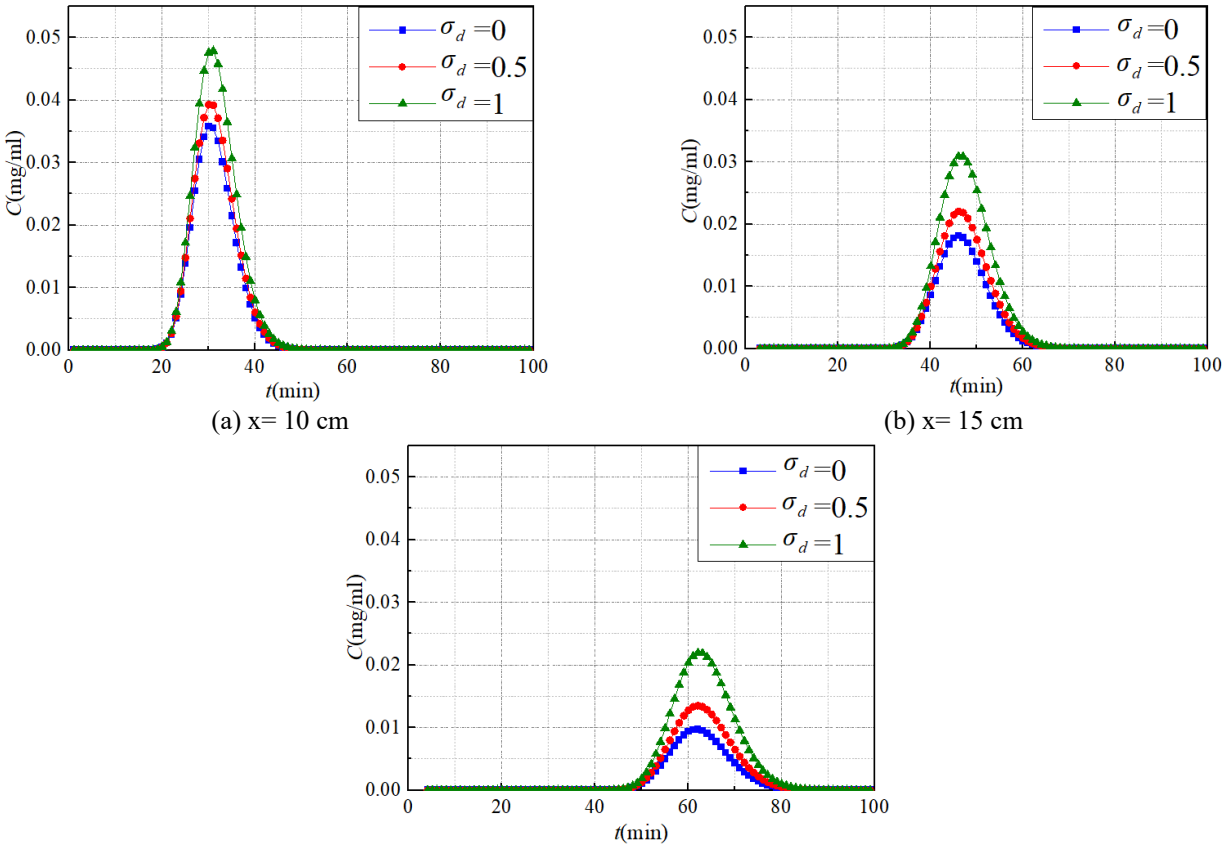

(a) x= 10 cm (b) x= 15 cm

(c) x= 20 cm

Fig. 2 Variation of suspended particle concentration with elapsed time at different locations when k_d is stochastic

Table 1 Model parameters when the $\bar{k}_d$ is stochastic

Parameters	M/Q	v	D	$\bar{k}_d$	k_r
	(mg·min/cm^3)	(cm/min)	(cm^2/min)	(min^{-1})	(min^{-1})
value	1	0.313	0.0313	0.03	0.01

Table 2 Model parameters when the v is stochastic

Parameters	M/Q	$\bar{v}$	D	k_d	k_r
	(mg·min/cm^3)	(cm/min)	(cm^2/min)	(min^{-1})	(min^{-1})
value	1	0.313	0.0313	0.03	0.001

particle concentration with time at standard deviation σ_v are shown in Fig. 3.

When the pore water velocity obeys the lognormal distribution, with the increase of σ_v, the peak concentration decreases and the time corresponding to the concentration peak gets earlier, different from the deposition coefficient obeying the lognormal distribution law. Meanwhile, the BTCs of SPs tend to be more asymmetric. The distribution range of pore water velocity becomes broader as σ_v increases, and a certain amount of faster pore water velocity is distributed in the flow velocity distribution. The water flows with relatively faster velocity transport most of the SPs, therefore, the entire BTCs reach the peak concentration earlier. However, the average pore water velocity decreases due to the increase of σ_v, and the effect of hydrodynamic action on the migration of SPs in porous media decreases, leading to the decrease of the outflow peak concentration. Because of the broader distribution range of pore water velocity, the distribution of the BTCs is more dispersed, appearing a trailing tail. It takes longer time for the breakthrough curve to reach the peak concentration when migrating to a farther distance, and peak concentration decreases accordingly.

When the deposition coefficient obeys the bimodal lognormal distribution, it is assumed that there are two types of the deposition coefficient (i.e., high and low). The specific parameters are shown in the Table 3. The high deposition coefficient $\bar{k}_{d,high}$ is 20 times as great as the low deposition coefficient $\bar{k}_{d,low}$.

Supposing $\sigma_{low} = \sigma_{high} = 0.1$in the bimodal lognormal distribution function, the average pore water velocity v and the release coefficient k_r are assumed constant. The trends in Fig. 4 can be described by f_{low} in the Eq. (31). When the SPs migrate along the x-axis direction, the BTCs with time at x=10, 15, 20 cm with different f_{low} are shown in Fig. 4.

As we see in Fig. 4, there is no low deposition coefficient when $f_{low} = 0$, and the bimodal lognormal distribution degenerates into single lognormal distribution. In this case, $\bar{k}_d$ is very large (i.e., $\bar{k}_d = 0.3$ min^{-1}), thus the peak concentration is quite small. With the increase of f_{low}, the proportion of $\bar{k}_{d,low}$ increases, the mean value of the overall deposition coefficients decreases, and the peak

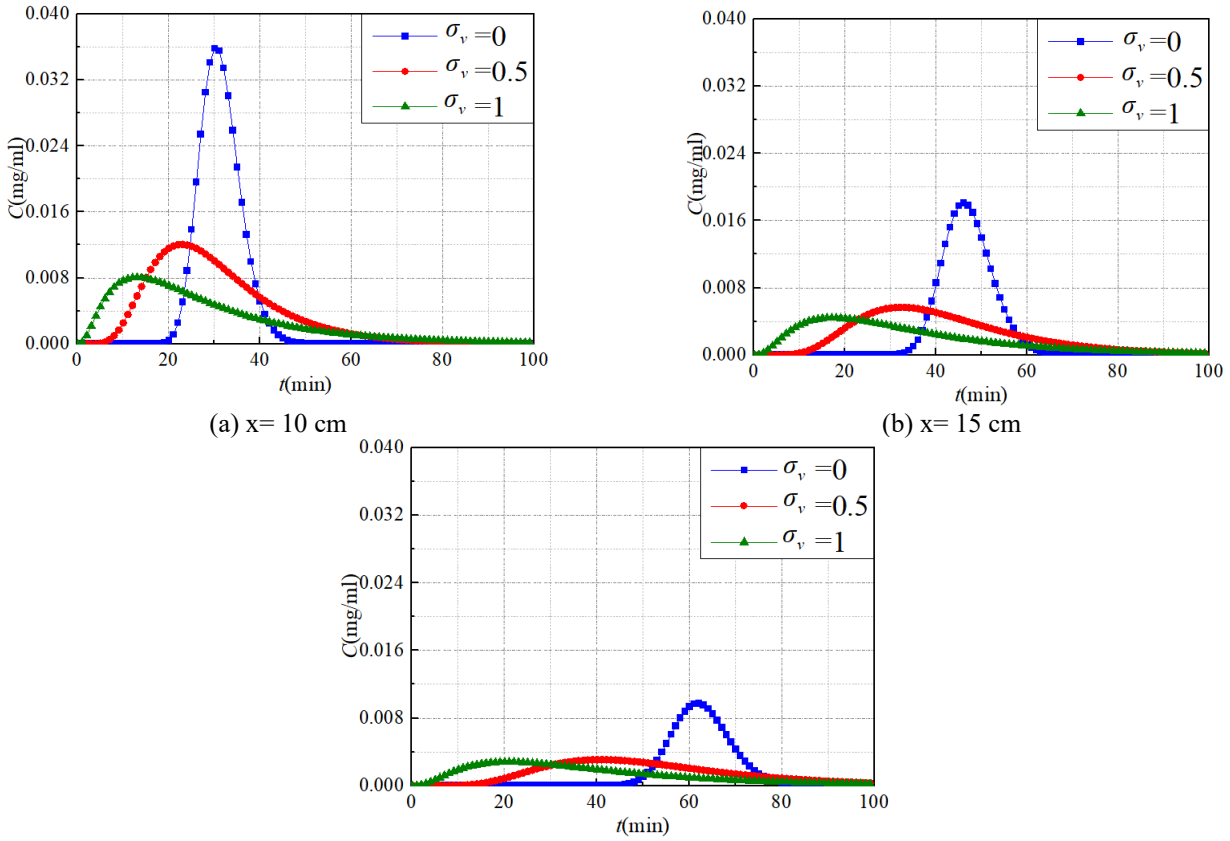

(a) x= 10 cm (b) x= 15 cm

(c) x= 20 cm

Fig. 3 Variation of suspended particle concentration with elapsed time at different locations when v is stochastic

Table 3 Model parameters when the k_d obeys the bimodal lognormal distribution

Parameters	M/Q	v	D	$\bar{k}_{d,low}$	$\bar{k}_{d,high}$	k_r
	(mg·min/cm^3)	(cm/min)	(cm^2/min)	(min^{-1})	(min^{-1})	(min^{-1})
value	1	0.313	0.0313	0.015	0.3	0.001

Table 4 Model parameters when the v obeys the bimodal lognormal distribution

Parameters	M/Q	$\bar{v}_{low}$	$\bar{v}_{high}$	D	$\bar{k}_{d,low}$	k_r
	(mg·min/cm^3)	(cm/min)	(cm/min)	(cm^2/min)	(min^{-1})	(min^{-1})
value	1	0.0313	0.313	0.0313	0.015	0.001

concentration increases and the concentration of SPs deposited in porous media decreases accordingly. When $f_{low} = 1$, there is only low deposition coefficient, in this situation, the peak concentration is the largest. As can be seen in the figure, the deposition coefficient has a great influence on the BTCs of SPs. With the SPs migrating to a far distance, the BTCs in Fig. 4 are similar to those in Fig. 2. As time elapses, the peak concentration decreases and the SPs migrate to a farther location. Because the meaning of release coefficient is opposite to that of deposition coefficient, the release coefficient obeys the law of bimodal normal distribution, which is opposite to that of deposition coefficient.

When the average pore water velocity follows the bimodal lognormal distribution, it is assumed that there are two types of pore water velocity (i.e., high and low). The specific parameters are shown in Table 4.

Supposing that $\sigma_{low} = \sigma_{high} = 0.1$ in the bimodal lognormal distribution function, and assuming that the deposition coefficient k_d and the release coefficient k_r are constant, the SPs migrate along the x-axis direction, the BTCs with time at x=10, 15, 20 cm with different f_{low} are shown in Fig. 5.

As shown in Fig. 5, the peak concentration changes with the variation of f_{low}, while the time corresponding to the peak concentration is almost unchanged because the value of $\bar{v}_{low}$ is too small. When $f_{low} = 1$, the peak concentration of SPs is almost zero, indicating that the pore water velocity is very slow, and almost all SPs are deposited in porous media. Thus, changing f_{low} has little effect on the time corresponding to the peak concentration. To prove this conclusion, assuming that $\bar{v}_{low}$ = 0.212 cm/min, and other parameters remain unchanged, the relationship between suspended particle concentration and time at x=10 cm are shown in Fig. 6. As increasing f_{low}, the proportion of $\bar{v}_{low}$ increases, and the average pore water velocity decreases, therefore, the SPs deposited in porous media increase, and the peak concentration of SPs decreases and the corresponding time increases, which is consistent with previous similar studies (Ahfir *et al*. 2007, *Ahfir et al*. 2017, Wang *et al.* 2017).

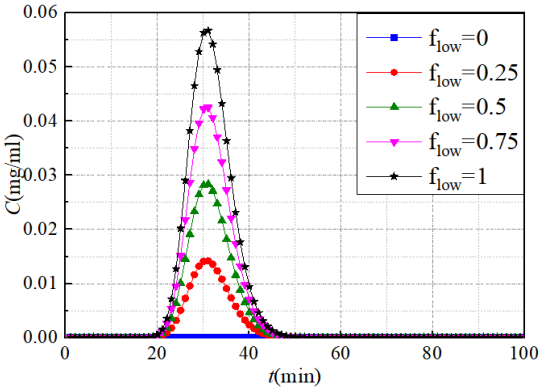

(a) x= 10 cm

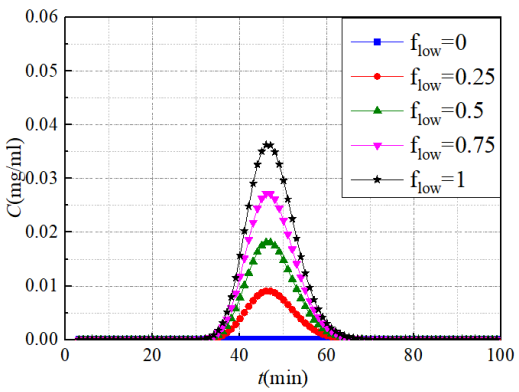

(b) x= 15 cm

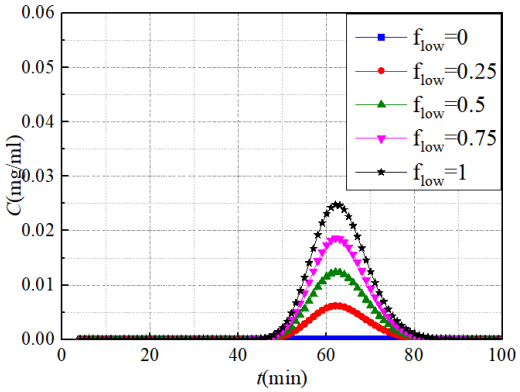

(c) x= 20 cm

Fig. 4 Relationship between suspended particle concentration and time at different locations when the k_d obeys the bimodal lognormal distribution

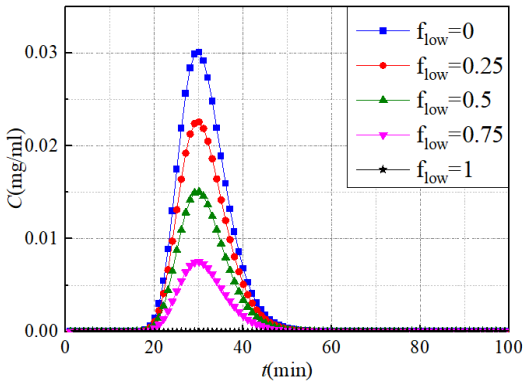

(a) x= 10 cm

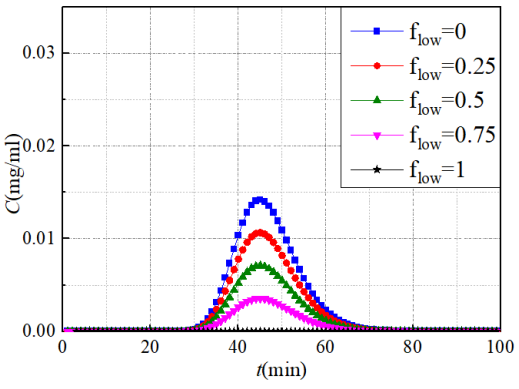

(b) x= 15 cm

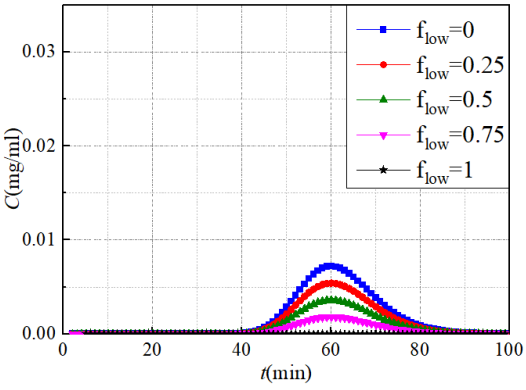

(c) x= 20 cm

Fig. 5 Relationship between suspended particle concentration and time at different locations when the v obeys the bimodal lognormal distribution

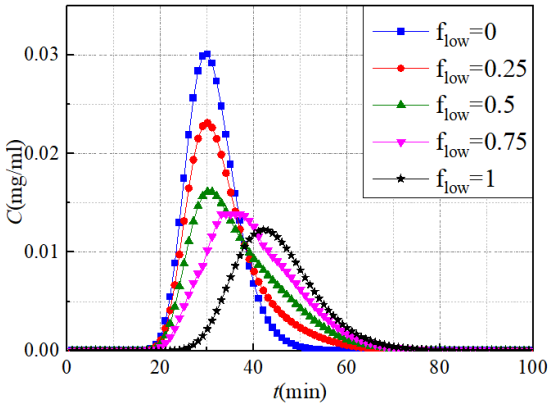

Fig. 6 Relationship between suspended particle concentration and time at x=10 cm when the $\bar{v}_{low}$ = 0.212 cm/min

Table 5 Model parameters when k_d and v obey the lognormal distribution

Parameters	M/Q	$\bar{v}$	D	$\bar{k}_d$	k_r	σ_v	σ_{vd}
	(mg·min/cm^3)	(cm/min)	(cm^2/min)	(min^{-1})	(min^{-1})	-	-
value	1	0.313	0.0313	0.03	0.001	1	1

When the time is fixed, the relationship between the concentration of SPs and the displacement is shown in Fig. 7, and the BTCs of SPs appear double peaks. When f_{low} = 0, the pore water velocity has no low term, therefore, there is only single peak. There is only a fast pore water velocity, thus, at any specific time, the maximum peak concentration occurs accordingly. When f_{low} =1, the pore water velocity has only a low term and the BTCs have only single peak, the minimum peak concentration occurs at the smallest corresponding migrating distance. When 0<f_{low}<1, the pore water velocity has two terms (i.e., low and high), double peaks appear accordingly. At any given time, with greater pore water velocity, the suspended particle can reach a farther location. With increasing f_{low}, the proportion of$\bar{v}_{low}$ increases, therefore, the peak concentration increases at nearer locations and decreases at farther locations. With time elapsing, the SPs migrate to farther locations, and more SPs deposit in the porous media, leading to smaller peak concentration of outflowing SPs.

When both the deposition coefficient and pore water velocity obey the lognormal distribution, the stochastic model is two-dimensional lognormal distribution. Assuming that the correlation coefficient ρ_{vd} = -1, -0.5, 0, 0.5, 1 and other parameters are constant, the specific parameters are shown in Table 5.

According to the physical meaning of the correlation coefficient, the lower correlation coefficient ρ_{vd} indicates the higher pore water velocity and the lower deposition coefficient. The relationship between suspended particle concentration and time at different locations is shown in Fig. 8. As ρ_{vd} decreases, the peak concentration tends to be larger since $\bar{v}_{high}$ and $\bar{k}_{d,low}$ can jointly promote the release and transport of SPs, resulting in relatively

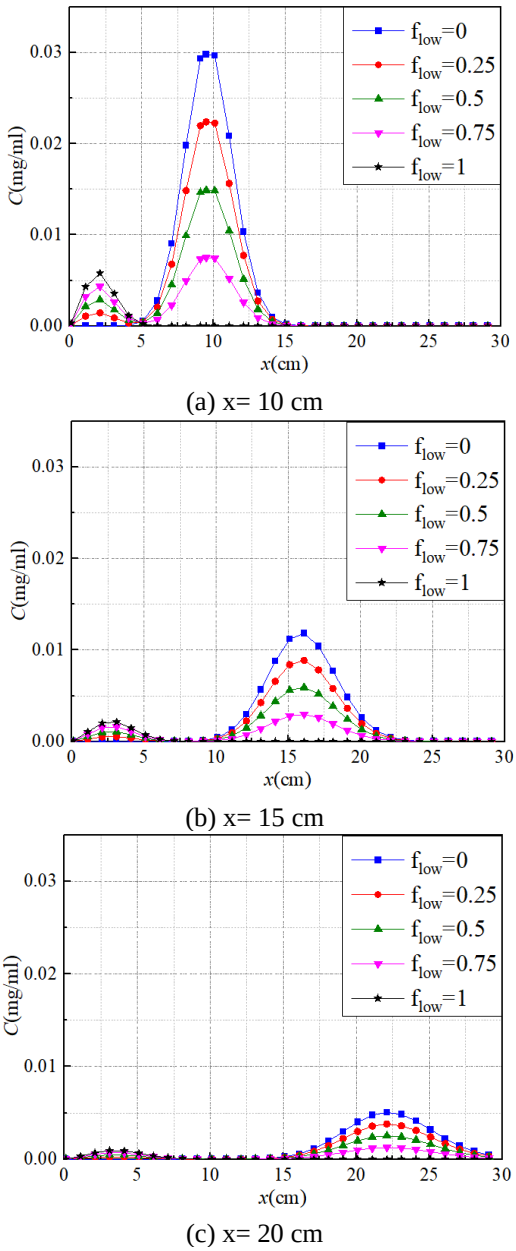

(a) x= 10 cm

(b) x= 15 cm

(c) x= 20 cm

Fig. 7 Relationship between suspended particle concentration and displacement at different times

symmetrical BTCs with less trailing phenomenon. As we can see from the peak concentrations of SPs in Figs. 8(a)-8(c), the concentration of deposited SPs is higher at the location closer to the upper surface. For instance, when ρ_{vd} = -1, the concentration of SPs decreases from 0.0098, 0.0059 to 0.0041 mg/mL at the location from 10, 15 to 20 cm, respectively, confirming that during the process of suspended particle migration, most SPs are deposited at the inlet, and decrease sequentially with depth in the form of hyper-exponential distribution.

5. Conclusions

Based on the advection-dispersion model of SPs taking the first-order kinetic deposition and the release of SPs into

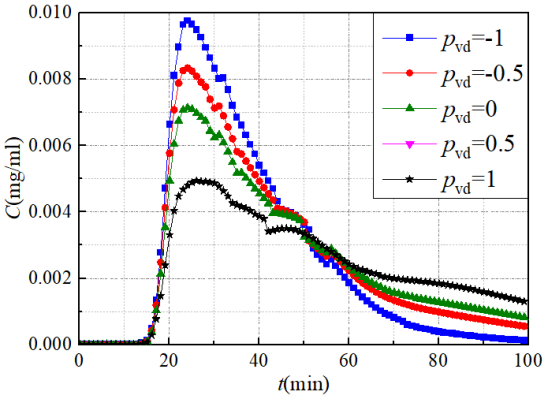

(a) x= 10 cm

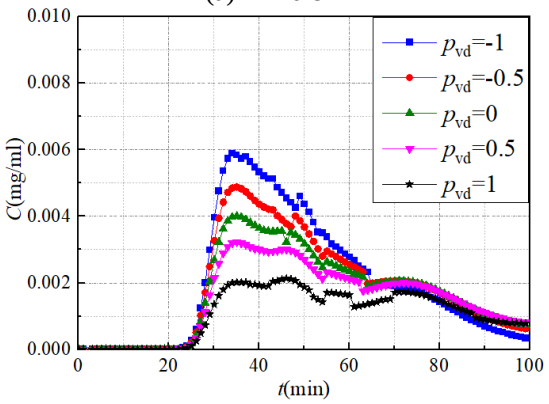

(b) x= 15 cm

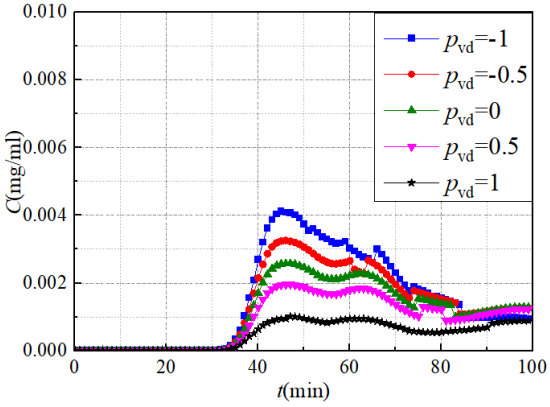

(c) x= 20 cm

Fig. 8 Relationship between suspended particle concentration and time at different locations when k_d and v obey the lognormal distribution

account, a stochastic model was introduced. One or two stochastic parameters (i.e., deposition coefficient, release coefficient, and average pore water velocity) were considered to study the migration of the SPs. The main conclusions are as follows:

• When the k_d follows the lognormal distribution, the mean value of k_d decreases with the σ_d increases of and causing the peak concentration of SPs increases. When v follows lognormal distribution, the BTCs of SPs become more asymmetric with the increase of σ_v, the peak concentration of SPs decreases and the corresponding time of peak concentration advances.

• When k_d follows the bimodal lognormal distribution, the peak concentration changes, significantly with different values of f_{low}, the peak concentration increases as f_{low} increases.

• When the v obeys the bimodal lognormal distribution, the value of $\bar{v}_{low}$ has a significant impact on the BTCs. Changing f_{low} only changes the peak concentration when $\bar{v}_{low}$ is small. While, when the value of $\bar{v}_{low}$ is reasonable, the peak concentration decreases and the corresponding time increases with increasing f_{low}.

• When both the deposition coefficient and pore water velocity follow the lognormal distribution, the peak concentration of SPs increases with the decrease of correlation coefficient ρ_{vd}, making the BTCs relatively symmetrical and with less trailing phenomenon.

• With the increase of migration distance, the time corresponding to the peak concentration of SPs increases and the peak concentration decreases in the BTCs. Moreover, the difference between the peak concentrations decreases.

Although the models presented here have advantages due to their analytical nature, they have some limitations, such as (a) the inability to account for gravity effects affect; and (b) the neglect of SPs aggregation. Nevertheless, the introduction of these stochastic parameters is essential for understanding the migration processes of SPs in porous media, serving as a foundation for validating more complex numerical models.

Acknowledgments

We would like to express our sincere gratitude for the financial support of the National Natural Science Foundation of China (grant 51678311) to this study. We also sincerely thank the reviewers for their helpful and constructive suggestions and the editors for their careful and patient work.

References

Abdel-Salam, A. and Chrysikopoulos, C.V. (1994), "Analytical solutions for one-dimensional colloid transport in saturated fractures", *Adv. Water Resour.*, **17**, 283-296. https://doi.org/10.1016/0309-1708(94)90032-93.

Ahfir, N., Benamar, A., Alem, A. and Wang, H. (2009), "Influence of internal structure and medium length on transport and deposition of suspended particles: A laboratory study", *Transport in Porous Media*, **76**, 289-307. https://doi.org/10.1007/s11242-008-9247-3.

Ahfir, N., Hammadi, A., Alem, A., Wang, H., Le Bras, G. and Ouahbi, T. (2017), "Porous media grain size distribution and hydrodynamic forces effects on transport and deposition of suspended particles", *J. Environ. Sci.*, **53**, 161-172. https://doi.org/10.1016/j.jes.2016.01.032.

Ahfir, N., Wang, H.Q., Benamar, A., Alem, A., Massei, N. and Dupont, J. (2007), "Transport and deposition of suspended particles in saturated porous media: hydrodynamic effect", *Hydrogeol. J.*, **15**, 659-668. https://doi.org/10.1007/s10040-006-

0131-3.
Babakhani, P., Bridge, J., Doong, R. and Phenrat, T. (2017), "Continuum-based models and concepts for the transport of nanoparticles in saturated porous media: A state-of-the-science review", *Adv. Colloid Interfac*., **246**, 75-104. https://doi.org/10.1016/j.cis.2017.06.002.
Bai, B., Jiang, S., Liu, L., Li, X. and Wu, H. (2021), "The transport of silica powders and lead ions under unsteady flow and variable injection concentrations", *Powder Technol*., **387**, 22-30. https://doi.org/10.1016/j.powtec.2021.04.014.
Bai, B., Xu, T. and Guo, Z. (2016), "An experimental and theoretical study of the seepage migration of suspended particles with different sizes", *Hydrogeol. J*., **24**, 2063-2078. https://doi.org/10.1007/s10040-016-1450-7.
Bai, B., Long, F., Rao, D. and Xu, T. (2017), "The effect of temperature on the seepage transport of suspended particles in a porous medium", *Hydrolog. Processes*, **31**, 382-393. https://doi.org/10.1002/hyp.11034.
Benamar, A., Ahfir, N., Wang, H. and Alem, A. (2007), "Particle transport in a saturated porous medium: Pore structure effects", *Comptes Rendus Geosci.*, **339**, 674-681. https://doi.org/10.1016/j.crte.2007.07.012.
Bradford, S.A., Morales, V.L., Zhang, W., Harvey, R.W., Packman, A.I., Mohanram, A. and Welty, C. (2013), "Transport and fate of microbial pathogens in agricultural settings", *Critical reviews in environmental science and technology*, **43**, 775-893. http://doi.org/10.1080/10643389.2012.710449.
Bradford, S.A. and Leij, F.J. (2018), "Modeling the transport and retention of polydispersed colloidal suspensions in porous media", *Chem. Eng. Sci*., **192**, 972-980. https://doi.org/10.1016/j.ces.2018.08.037.
Bradford, S.A. and Toride, N. (2007), "A stochastic model for colloid transport and deposition", *J. Environ Quality*, **36**, 1346-1356. https://doi.org/10.2134/jeq2007.0004.
Braga, A.S. and Filion, Y. (2022), "The interplay of suspended sediment concentration, particle size and fluid velocity on the rapid deposition of suspended iron oxide particles in PVC drinking water pipes", *Water Research X*, 15. https://doi.org/10.1016/j.wroa.2022.100143.
Chen, X., Cai, Q. and Wu, Z. (2017), "Experimental and theoretical study of coupled influence of flow velocity increment and particle size on particle retention and release in porous media", *Water Sci. Eng*., **10**, 236-245. https://doi.org/10.1016/j.wse.2017.10.004.
Cui, D., Li, A. and Ren, X, (2019), "Experimental study on the impacts of suspended solid particles in the reinjection water on the reservoir damage", *IOP conference series, Earth and environmental science*, **252**, 52155. https://doi.org/10.1088/1755-1315/252/5/052155.
Cui, G., Ning, F. and Dou, B. (2022), "Particle migration and formation damage during geothermal exploitation from weakly consolidated sandstone reservoirs via water and CO2 recycling", *Energy*, **240**, 122507. https://doi.org/10.1016/j.energy.2021.122507.
Ding, Y., Jia, Y., Wang, X., Zhang, J., Luo, H., Zhang, Y. and Chen, X. (2022), "The characteristics of subgrade mud pumping under various water level conditions", *Geomech. Eng*., **30**(2), 201-210. https://doi.org/10.12989/gae.2022.30.2.201.
Dong, Z., Qiu, Y., Zhang, W., Yang, Z. and Wei, L. (2018), "Size-dependent transport and retention of micron-sized plastic spheres in natural sand saturated with seawater", *Water Res.*, **143**, 518-526. https://doi.org/10.1016/j.watres.2018.07.007.
Haque, M.E., Shen, C., Li, T., Chu, H., Wang, H., Li, Z. and Huang, Y. (2017), "Influence of biochar on deposition and release of clay colloids in saturated porous medi", *J. Environ. Quality*, **46**, 1480-1488. https://doi.org/10.2134/jeq2017.06.0223.
Hosseini, S.M. and Tosco, T. (2013), "Transport and retention of high concentrated nano-Fe/Cu particles through highly flow-rated packed sand column", *Water Res.*, **47**, 326-338. https://doi.org/10.1016/j.watres.2012.10.002.
Hossini, H., Shafie, B., Niri, A.D., Nazari, M., Esfahlan, A.J., Ahmadpour, M., Nazmara, Z, Ahmadimanesh, M., Makhdoumi, P., Mirzaei, N. and Hoseinzadeh, E. (2022), "A comprehensive review on human health effects of chromium: insights on induced toxicity", *Environ. Sci. Pollut. Res*., **29**, 70686-70705. https://doi.org/10.1007/s11356-022-22705-6.
James, S.C. and Chrysikopoulos, C.V. (2003), "Analytical solutions for monodisperse and polydisperse colloid transport in uniform fractures", *Colloids and Surfaces A: Physicochemical and Engineering Aspects*, **226**, 101-118. https://doi.org/10.1016/S0927-7757(03)00316-9.
Johnson, W.P., Rasmuson, A., Pazmiño, E. and Hilpert, M. (2018), "Why variant colloid transport behaviors emerge among identical individuals in porous media when colloid–surface repulsion exist", *Environ. Sci. Technol*., **52**, 7230-7239. https://doi.org/10.1021/acs.est.8b00811.
Johnson, W.P., Rasmuson, A., Ron, C., Erickson, B., VanNess, K., Bolster, D. and Peters, B. (2020), "Anionic nanoparticle and microplastic non-exponential distributions from source scale with grain size in environmental granular media", *Water Res.*, **182**, 116012. https://doi.org/10.1016/j.watres.2020.116012.
Katzourakis, V.E. and Chrysikopoulos, CV. (2019), "Two-site colloid transport with reversible and irreversible attachment: Analytical solutions", *Adv. Water Resour.*, **130**, 29-36. https://doi.org/10.1016/j.advwatres.2019.05.0262.
Lin, D., Hu, L., Bradford, S.A., Zhang, X. and Lo, I.M.C. (2022), "Prediction of collector contact efficiency for colloid transport in porous media using Pore-Network and Neural-Network models", *Separation and Purification Technology*, **290**, 120846. https://doi.org/10.1016/j.seppur.2022.120846.
Ma, C., Huangfu, X., He, Q., Ma, J. and Huang, R. (2018), "Deposition of engineered nanoparticles (ENPs) on surfaces in aquatic systems: a review of interaction forces, experimental approaches, and influencing factors", *Environ. Sci. Pollution Res.*, **25**, 33056-33081. https://doi.org/10.1007/s11356-018-3225-2.
Qi, K., Lu, N., Zhang, S., Wang, W., Wang, Z. and Guan, J. (2021), "Uptake of Pb(II) onto microplastic-associated biofilms in freshwater: Adsorption and combined toxicity in comparison to natural solid substrates", *J. Hazard. Mater*., **411**, 125115. https://doi.org/10.1016/j.jhazmat.2021.125115.
Shapiro, A.A. and Bedrikovetsky, P.G. (2010), "A stochastic theory for deep bed filtration accounting for dispersion and size distributions", *Physica A: Statistical Mech. Appl*., **389**, 2473-2494. https://doi.org/10.1016/j.physa.2010.02.049.
Sim, Y. and Chrysikopoulos, C.V. (1998), "Analytical solutions for solute transport in saturated porous media with semi-infinite or finite thickness", *Transport in Porous Media*, **30**, 87-112.
Sim, Y. and Chrysikopoulos, C.V. (1999), "Three-dimensional analytical models for virus transport in saturated porous media", *Adv. Water Resour*., **22**(5), 507-519. https://doi.org/10.1016/S0309-1708(98)00027-X.
Taghavy, A., Kim, I., Huh, C. and DiCarlo, D.A. (2018), "A two-site filtration model for silica nanoaggregate mobility in porous media under high salinity conditions", *J. Nanoparticle Res*., **20**, 1-12. https://doi.org/10.1007/s11051-018-4250-2.
Tufenkji, N. and Elimelech, M, (2005a), "Spatial distributions of cryptosporidium oocysts in porous media: Evidence for dual mode deposition", *Environ. Sci. Technol*., **39**, 3620-3629. https://doi.org/10.1021/es048289y.
Tufenkji, N. and Elimelech, M. (2004), "Deviation from the classical colloid filtration theory in the presence of repulsive DLVO interactions", *Langmuir*, **20**, 10818-10828.

http://doi.org/10.1021/la0486638.
Tufenkji, N. and Elimelech, M. (2005b), "Breakdown of colloid filtration theory: Role of the secondary energy minimum and surface charge heterogeneities", *Langmuir*, **21**, 841-852. https://doi.org/10.1021/la048102g.
Tufenkji, N., Redman, J.A. and Elimelech, M. (2003), "Interpreting deposition patterns of microbial particles in laboratory-scale column experiments", *Environ. Sci. Technol*., **37**, 616-623. https://doi.org/10.1021/es025871i.
Wang, F., Li, Z. and Huai, W. (2022), "A random displacement model of sediment transport in ice-covered alluvial channel flows", *Environ. Sci. Pollut. Res*., **29**(46), 70099-70113. https://doi.org/10.1007/s11356-022-20833-7.
Wang, M., Gao, B., Tang, D., Sun, H., Yin, X. and Yu, C. (2017), "Effects of temperature on graphene oxide deposition and transport in saturated porous media", *J. Hazardous Mater*., **331**, 28-35. https://doi.org/10.1016/j.jhazmat.2017.02.014.
Wang, Z., Du, X., Yang, Y. and Ye, X. (2012), "Surface clogging process modeling of suspended solids during urban stormwater aquifer recharge", *J. Environ. Sci*. (China), **24**, 1418-1424. https://doi.org/10.1016/S1001-0742(11)60961-3.
Yuan, H. and Sin, G. (2011), "Uncertainty and sensitivity analysis of filtration models for non-Fickian transport and hyperexponential deposition", *Chem. Eng. J*., **168**(2), 635-648. https://doi.org/10.1016/j.cej.2011.01.051.
Zhu, B., Tang, H., Yin, S., Chen, G., Zhao, F. and Xu, S. (2021), "Effect of fracture roughness on transport of suspended particles in fracture during drilling", *J. Petroleum Sci. Eng*., **207**, 109080. https://doi.org/10.1016/j.petrol.2021.109080.
Zou, Z., Shu, L., Min, X, and Mabedi, E.C. (2019a), "Physical experiment and modeling of the transport and deposition of polydisperse particles in stormwater: effects of a depth-dependent initial filter coefficient", *Water*, **11**(9), 1885. https://doi.org/10.3390/w11091885.
Zou, Z., Shu, L., Min, X. and Mabedi, E.C. (2019b), "Clogging of infiltration basin and its impact on suspended particles transport in unconfined sand aquifer: insights from a laboratory study", *Water*, **11**(5), 1083. https://doi.org/10.3390/w11051083.

CC